Asociación Argentina de Mecánica Computacional

Mecánica Computacional Vol XXV, pp. 1751-1765
Alberto Cardona, Norberto Nigro, Victorio Sonzogni, Mario Storti. (Eds.)
Santa Fe, Argentina, Noviembre 2006

NON LINEAR MODEL FOR COUPLED VIBRATIONS OF DRILL-STRINGS

Marcelo T. Piovan[a] **and Rubens Sampaio**[b]

[a]*Mechanical Systems Analysis Group, Universidad Tecnológica Nacional - Fac. Reg. Bahía Blanca, 11 de Abril 461, Bahía Blanca, BA, 8000, Argentina, e-mail: mpiovan@frbb.utn.edu.ar,*
`http://www.frbb.utn.edu.ar`

[b]*Department of Mechanical Engineering, Pontifícia Universidade Católica - Rio de Janeiro, Rua Marquês de São Vicente 225, Rio de Janeiro, RJ, 22453-900, Brasil, e-mail: rsampaio@mec.puc-rio.br*
`http://www.mec.puc-rio.br`

Keywords: Drill-Strings, non-linear dynamics.

Abstract. In the present work a continuous model is presented to study, by means of finite element discretization, the coupling of extensional, flexural and torsional vibrations on a drillstring, which is described as a vertical slender beam under axial rotation. The structure is subjected to distributed loads due to its own weight, the reaction force and perturbation moments at the lower end. The beam structure is also confined to move inside a rigid cylinder, which simulates the borehole. The impacts and friction of the drill-string with the borehole are modeled employing simplified forms. It is known that the accounting of geometrical non-linearities affects the dynamics of slender beams. The vibrations of drill-strings are frequently analyzed by means of lumped parameter models. Normally, these models employ equivalent lumped parameters which are obtained from experimental field data or from continuous models assuming one-mode approximation for extensional, flexural and torsional vibrations. However, the lumped parameter models do not include dynamical effects due to geometrical non-linearities. In this context, the objective of present work is to analyze the effects of geometrical non-linearities in the vibration of drill-strings together with the patterns of vibroimpact and comparing the results with the predictions of linear models. The beam model is discretized using a finite element with 12 degrees of freedom. The results have shown an important influence of the geometric non-linearities (when compared with the predictions of a linear model) in the dynamic responses of the drill-strings, especially when the beam undergoes impact patterns with the borehole or the rock formation. This influence can be observed in the calculation of reaction forces at top position as well as the time histories of radial displacements..

1 INTRODUCTION

The presence of intense vibrations in a drill-string has been considered for many years as one of the most relevant causes of loss of performance in the drilling process. In the oil industry, the improvement of drilling performance is a matter of crucial economical interest, consequently the analysis of drill-string vibrations was the subject of many investigations as reported in the specialized literature (Jansen, 1991; Jansen and van den Steen, 1995; Tucker and Wang, 1999; Chen and Géradin, 1995; Khulief and Al-Naser, 2005). It was observed that the drill-string vibrations become more severe in the bottom-hole assemblies, due to the presence of compression. The main cause of vibrations in the drill-string is due to contact of the driving pipes and the impact of the bottom-hole assemblies with the borehole. Also the misalignment of the pipes is another cause for drill-string vibrations (Khulief and Al-Naser, 2005). In general, the dynamic pattern of these vibrations includes coupling of axial, flexural and torsional deformations. Although many researchers made attempts to simplify the problem by employing lumped parameter models (Yigit and Christoforou, 1998, 2000; Christoforou and Yigit, 2003) or simplified continuous models which consider only axial/flexural vibrations (Trindade et al., 2005) or axial/torsional (Sampaio et al., 2005), it is only recently that the treatment of drilling assemblies, as an integrated system, has been taken into account (Tucker and Wang, 1999, 2003).

Vibrations of drill-strings are often analyzed by means of discrete or lumped parameter models (Yigit and Christoforou, 2000; Richard et al., 2004) taking into account non-linear forces/torques interactions with the rock formation. These models allow the study of a complex problem by connecting lumped masses and springs, among others, in a conceptually simplified fashion which also facilitate the implementation of control schemes. Yigit and Christoforou developed a lumped parameter model with the scope to analyze the coupled torsional/flexural vibrations of drill-strings. They analyzed qualitatively and quantitatively the vibrations of the drill-string and employed a linear scheme to control the oscillations (Yigit and Christoforou, 2000). These authors extended (Christoforou and Yigit, 2003) their previous work to include also axial coupling by means of a simplified ordinary differential equation in the axial direction. Other authors analyzed the self-excited stick-slip vibrations of drill-strings (Richard et al., 2004) by means of a simplified lumped parameter model, which accounts for torsional and extensional motions coupled in the boundary. Recently, a non-linear continuous beam model to study the influence of geometrical non-linearities in coupled axial/transversal vibrations of drill-strings was introduced (Trindade et al., 2005). The rotordynamics theory together with the finite element method (Khulief and Al-Naser, 2005; Berlioz et al., 1996; Melakhessou et al., 2003) was employed to develop dynamic models for drill-strings. Although in these last models gyroscopic effects, among others were taken into account, the effect of initial stresses was considered in a simplified form (Khulief and Al-Naser, 2005).

It is interesting to note that finite element procedures were used to study the drill-strings and many of the reported research have addressed only the study of the Bottom-Hole-Assemblies, BHA (Chen and Géradin, 1995; Khulief and Al-Naser, 2005). However the features of a drill-string structure subjected to the state of initial stresses (with the upper part under tension and lower under compression) have not been analyzed within a general continuous model accounting for axial, flexural and torsional coupled motions. In this context the authors believe that the appropriate analysis of drill-strings vibrations has to be done with more realistic continuous models incorporating geometric non-linearities, impacts and gyroscopic effects, among others.

In the present article, the coupled axial, flexural and torsional vibrations of drill-strings are studied by means of a non-linear beam model. The drill-string is subjected to a state of initial stresses, leading to geometrical stiffening in the upper part due to tension and softening of its lower part due to compression when the bit is acting. The finite element method is employed to discretize the continuous model to study the vibration patterns of the non-linear model. Comparisons of the responses of the non-linear model with those of a linear model in several operative conditions are carried out. A linear model can be obtained from the non-linear, neglecting the geometric non-linearities. The discretization is carried out by means of a finite element with 12 degrees of freedom. In this work, it was shown that the predictions obtained with non-linear model have strong quantitative and qualitative discrepancies with respect to the predictions of the linear model, especially when the drill-string undergo impact patterns. These differences are due to geometric coupling among the axial, flexural and torsional vibrations present in the non-linear model and not in the linear one.

2 THE DRILL-STRING MODEL

Let us consider an initially straight slender rotating beam with annular cross-section (R_o and R_i are the outer and inner radii), and of length L in the undeformed state, as shown in the Figure 1. The beam is referred to an inertial cartesian system *O:XYZ* fixed to the undeformed beam. Another cartesian reference system *O:xyz* measures the deformation and displacements of the beam. In Figure 2, it is possible to see that the system *O:xyz* is rotated with respect to the system *O:XYZ* by means of a typical sequence of rotation angles as usual in rotordynamics (Gubran and Gupta, 2005; Mohiuddin and Khulief, 1999; Lalanne and Ferraris, 1990).

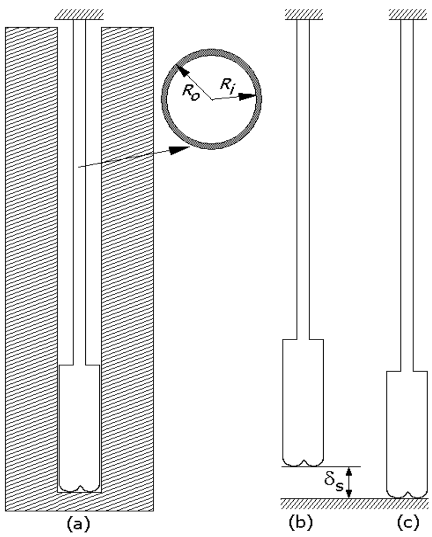

Figure 1: Drill String Scheme. (a) Description (b) Undeformed Configuration (c) Deformed Configuration

The beam is constructed with an homogeneous material and due to the the slenderness ratio (Length/Diameter) of the beam, Bernoulli-Euler assumptions are taken into account, i.e. the cross-section is rigid in its own-plane, and the transverse shear strains in the cross-section are negligible.

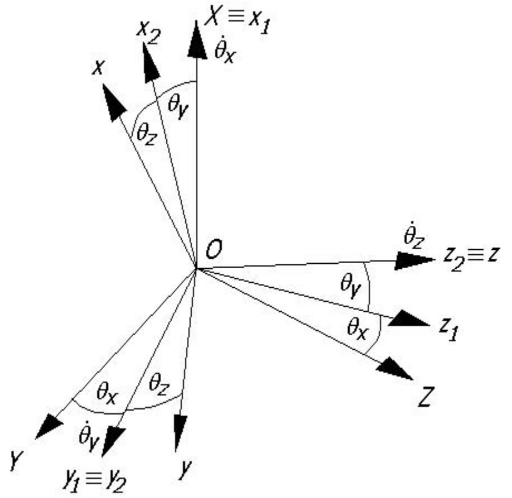

Figure 2: Reference systems and rotation angles

2.1 Kinetic and Strain Energies

The instantaneous angular velocity vector ω in the rotating frame can be expressed (Lalanne and Ferraris, 1990) as:

$$\omega = \dot{\theta}_x X + \dot{\theta}_y y_1 + \dot{\theta}_z z_2 \tag{1}$$

Transforming the expression (1) into the fixed reference system *O:XYZ*, and considering that the bending angles θ_y and θ_z are small (because the beam is constrained to move in a confined surface), then it is possible to obtain the rotational vector as:

$$\omega = \begin{Bmatrix} \omega_x \\ \omega_y \\ \omega_z \end{Bmatrix} = \begin{Bmatrix} \dot{\theta}_x - \dot{\theta}_z \theta_y \\ \dot{\theta}_y \cos\theta_x - \dot{\theta}_z \sin\theta_x \\ \dot{\theta}_y \sin\theta_x + \dot{\theta}_z \cos\theta_x \end{Bmatrix} \tag{2}$$

The kinetic energy can be expressed in the following form (Lalanne and Ferraris, 1990):

$$K = \frac{1}{2}\int_0^L \int_A \left(\dot{\boldsymbol{R}}^T \dot{\boldsymbol{R}}\right) dA dx = \frac{1}{2}\int_0^L \left[\rho A(x) \dot{\boldsymbol{r}}_0^T \dot{\boldsymbol{r}}_0 + \rho \omega^T \boldsymbol{I}(x)\omega\right] dx \tag{3}$$

where $\dot{\boldsymbol{R}}$ is the velocity of the position vector of a generic point of the cross-section, $\dot{\boldsymbol{r}}_0$ identifies the translational velocity of the cross-section, $\boldsymbol{I}(x)$ is the tensor of inertia (which is a diagonal matrix $\boldsymbol{I} = diag\,[2I(x), I(x), I(x)]$ because the moments of inertia are calculated with respect to the principal axes of inertia of the structural system).

Now, taking into account that, from the Bernoulli-Euler hypotheses for the bending angles, one has $\theta_z = v'$, $\theta_y = -w'$, and with:

$$\dot{\boldsymbol{r}}_0 = \{\dot{u}, \dot{v}, \dot{w}\}^T \tag{4}$$

then, substituting (2) and (4) into (3) and after a few algebraic manipulation, the kinetic energy can be written as:

$$K = \frac{1}{2}\int_0^L \left[\rho A\left(\dot{u}^2 + \dot{v}^2 + \dot{w}^2\right) + \rho I\left(\dot{v}'^2 + \dot{w}'^2\right) + \rho I_0 \dot{\theta}_x^2 + 2\rho I_0 \dot{\theta}_x \dot{v}' w'\right] dx \tag{5}$$

Where, $\rho A\dot{u}^2$, $\rho A\dot{v}^2$ and $\rho A\dot{w}^2$ are the translational terms of the kinetic energy, $\rho I_0\dot{\theta}_x^2$ is the kinetic energy due to the twisting motion, $\rho I\dot{w}'^2$ and $\rho I\dot{v}'^2$ are the terms corresponding to the bending rotations. Finally, the last term of (5) corresponds to the kinetic energy of the gyroscopic effect. Note that in the previous expressions, the primes and the points mean derivation with respect to the spatial variable x and the time t, respectively.

The strain energy, in the context of a beam theory, can be expressed as:

$$H = \frac{1}{2}\int_V \left[E\varepsilon_{xx}^2 + 4G\varepsilon_{xy}^2 + 4G\varepsilon_{xz}^2\right] dV \tag{6}$$

where the strains can be written as:

$$\begin{aligned}
\varepsilon_{xx} &= \frac{\partial u_x}{\partial x} + \frac{1}{2}\left(\frac{\partial u_x}{\partial x}\frac{\partial u_x}{\partial x} + \frac{\partial u_y}{\partial x}\frac{\partial u_y}{\partial x} + \frac{\partial u_z}{\partial x}\frac{\partial u_z}{\partial x}\right)\\
\varepsilon_{xy} &= \frac{1}{2}\left(\frac{\partial u_x}{\partial y} + \frac{\partial u_y}{\partial x} + \frac{\partial u_x}{\partial x}\frac{\partial u_x}{\partial y} + \frac{\partial u_y}{\partial x}\frac{\partial u_y}{\partial y} + \frac{\partial u_z}{\partial x}\frac{\partial u_z}{\partial y}\right)\\
\varepsilon_{xz} &= \frac{1}{2}\left(\frac{\partial u_x}{\partial z} + \frac{\partial u_z}{\partial x} + \frac{\partial u_x}{\partial x}\frac{\partial u_x}{\partial z} + \frac{\partial u_y}{\partial x}\frac{\partial u_y}{\partial z} + \frac{\partial u_z}{\partial x}\frac{\partial u_z}{\partial z}\right)
\end{aligned} \tag{7}$$

which can be expressed in terms of the displacement variables in the following form:

$$\begin{aligned}
\varepsilon_{xx} &= (u' - yv'' + zw'') + \frac{1}{2}\left[(u' - yv'' + zw'')^2 + (v' - z\theta_x')^2 + (w' + y\theta_x')^2\right]\\
\varepsilon_{xy} &= \frac{1}{2}\left[-v'(u' - yv'' + zw'') + (w' + y\theta_x')\,\theta_x - z\theta_x'\right]\\
\varepsilon_{zy} &= \frac{1}{2}\left[-w'(u' - yv'' + zw'') + (v' - z\theta_x')\,\theta_x + y\theta_x'\right]
\end{aligned} \tag{8}$$

Substituting (8) into (6) and integrating in the area, one obtains the strain energy expression of the beam in terms of the displacements. However, in the present work, only the contributions of cubic and lower order terms of u', v', w' and θ' in strain energy are retained. Thus, the simplified expression of the strain energy H, H_S, can described in the following form:

$$\begin{aligned}
H_S = \; & \frac{1}{2}\int_0^L \left\{EAu'^2 + EI\left(v''^2 + w''^2\right) + GI_0\theta_x'^2\right\} dx + \\
& \underline{\frac{1}{2}\int_0^L \left\{GI_0\left(v''w' - v'w''\right)\theta_x' + EA\left(u'^3 + u'v'^2 + u'w'^2\right)\right\} dx +}\\
& \underline{\frac{1}{2}\int_0^L \left\{EI_0\left(v'w'' - v''w' + \theta_x'u'\right)\theta_x' + 3EIu'\left(v''^2 + w''^2\right)\right\} dx}
\end{aligned} \tag{9}$$

The equation (9) has three integral terms. The first one corresponds to the linear components of the simplified strain energy, whereas the underlined terms corresponds to the non-linear components of the simplified strain energy.

The beam is subjected to its own weight, and the external work done by a vertical force due to gravity field can be expressed as (Trindade et al., 2005):

$$W = \int_0^L (\rho g A)\, u\, dx \tag{10}$$

2.2 Finite Element Formulation

The finite element model is obtained by means of the discretization of the equations of strain (9) and kinetic (5) energies and the equation of gravity forces (10), applying then the variational calculus to the discretized equations.

The discretization is carried out using Lagrange linear shape functions for the axial displacement u and twisting angle θ_x and Hermite cubic polynomials for the lateral displacements v and w. Thus, the displacements are discretized by means of the following expressions

$$u = \mathbf{N}_u \mathbf{q}_e \quad v = \mathbf{N}_v \mathbf{q}_e \quad w = \mathbf{N}_w \mathbf{q}_e \quad \theta_x = \mathbf{N}_\theta \mathbf{q}_e \tag{11}$$

where defining the element length with l_e, and the non-dimensional element variable $\xi = x/l_e$:

$$\begin{aligned}
\mathbf{N}_u &= \{1-\xi, 0, 0, 0, 0, 0, \xi, 0, 0, 0, 0, 0\} \\
\mathbf{N}_v &= \{0, 1-3\xi^2+2\xi^3, l_e\xi(1-\xi)^2, 0, 0, 0, 0, \xi^2(3-2\xi), l_e\xi^2(\xi-1), 0, 0, 0\} \\
\mathbf{N}_w &= \{0, 0, 0, 1-3\xi^2+2\xi^3, l_e\xi(1-\xi)^2, 0, 0, 0, 0, \xi^2(3-2\xi), l_e\xi^2(\xi-1), 0\} \\
\mathbf{N}_\theta &= \{0, 0, 0, 0, 0, 1-\xi, 0, 0, 0, 0, 0, \xi\} \\
\mathbf{q}_e^T &= \{u_1, v_1, v_1', w_1, w_1', \theta_{x1}, u_2, v_2, v_2', w_2, w_2', \theta_{x2}\}
\end{aligned} \tag{12}$$

In order to obtain the finite element equation, the following variational expression of the Hamilton's principle for a generic element:

$$\delta \int_{t_1}^{t_2} \left(K^{(e)} - H_S^{(e)} + W^{(e)} \right) dt = 0 \tag{13}$$

Then the discretized displacements (12) are introduced in each one of the energy terms of (13) and after performing the common steps of variational calculus in the corresponding discretized expressions of strain and kinetic energies and the gravity forces of the generic element, one obtains the following discretized expression:

$$\mathbf{M}^{(e)} \ddot{\mathbf{q}}_e + \mathbf{G}^{(e)} \dot{\mathbf{q}}_e + \left[\mathbf{K}_e^{(e)} + \mathbf{K}_g^{(e)} (\mathbf{q}_e) \right] \mathbf{q}_e = \mathbf{F}_g \tag{14}$$

where $\ddot{\mathbf{q}}_e$ and $\dot{\mathbf{q}}_e$ are the acceleration and velocity vectors of the generic element, respectively; whereas $\mathbf{M}^{(e)}$, $\mathbf{G}^{(e)}$, $\mathbf{K}_e^{(e)}$ and $\mathbf{K}_g^{(e)}$ are the mass matrix, gyroscopic matrix, elastic stiffness matrix and geometric stiffness matrix of the generic element, respectively. Whereas $\mathbf{F}_g$ is the vector for the gravity forces of the element. These matrices and vector are given by the following expressions:

$$\begin{aligned}
\mathbf{M}^{(e)} = & \int_0^1 \left[\rho A l_e \left(\mathbf{N}_u^T \mathbf{N}_u + \mathbf{N}_v^T \mathbf{N}_v + \mathbf{N}_w^T \mathbf{N}_w \right) \right] d\xi + \\
& \int_0^1 \left[\rho I_0 l_e \mathbf{N}_\theta^T \mathbf{N}_\theta + \frac{\rho I}{l_e} \left(\mathbf{N}_v'^T \mathbf{N}_v' + \mathbf{N}_w'^T \mathbf{N}_w' \right) \right] d\xi
\end{aligned} \tag{15}$$

$$\mathbf{G}^{(e)} = \int_0^1 \left[\frac{\omega^e \rho I_0}{l_e} \left(\mathbf{N}_w'^T \mathbf{N}_v' - \mathbf{N}_v'^T \mathbf{N}_w' \right) \right] d\xi \tag{16}$$

$$\begin{aligned} \mathbf{K}_e^{(e)} = \; & \int_0^1 \left[\frac{EA}{l_e} \mathbf{N}_u'^T \mathbf{N}_u' + \frac{GI_0}{l_e} \mathbf{N}_\theta'^T \mathbf{N}_\theta' \right] d\xi + \\ & \int_0^1 \left[\frac{EI}{l_e^3} \left(\mathbf{N}_v''^T \mathbf{N}_v'' + \mathbf{N}_w''^T \mathbf{N}_w'' \right) \right] d\xi \end{aligned} \tag{17}$$

$$\mathbf{F}_g = \int_0^1 \left[\rho g A l_e \mathbf{N}_u^T \right] d\xi \tag{18}$$

$$\begin{aligned} \mathbf{K}_g^{(e)} = \; & \int_0^1 \left[\frac{EA}{2l_e^2} \left(3\mathbf{N}_u'^T \mathbf{N}_u' \mathbf{q}_e \mathbf{N}_u' + \mathbf{N}_u'^T \mathbf{N}_v' \mathbf{q}_e \mathbf{N}_v' + \mathbf{N}_v'^T \mathbf{N}_v' \mathbf{q}_e \mathbf{N}_u' + \mathbf{N}_v'^T \mathbf{N}_u' \mathbf{q}_e \mathbf{N}_v' + \right) \right] d\xi + \\ & \int_0^1 \left[\frac{EA}{2l_e^2} \left(\mathbf{N}_u'^T \mathbf{N}_w' \mathbf{q}_e \mathbf{N}_w' + \mathbf{N}_w'^T \mathbf{N}_w' \mathbf{q}_e \mathbf{N}_u' + \mathbf{N}_w'^T \mathbf{N}_u' \mathbf{q}_e \mathbf{N}_w' \right) \right] d\xi + \\ & \int_0^1 \left[\frac{3EI}{2l_e^4} \left(\mathbf{N}_u'^T \mathbf{N}_v'' \mathbf{q}_e \mathbf{N}_v'' + \mathbf{N}_v''^T \mathbf{N}_v'' \mathbf{q}_e \mathbf{N}_u' + \mathbf{N}_v''^T \mathbf{N}_u' \mathbf{q}_e \mathbf{N}_v'' \right) \right] d\xi + \\ & \int_0^1 \left[\frac{3EI}{2l_e^4} \left(\mathbf{N}_u'^T \mathbf{N}_w'' \mathbf{q}_e \mathbf{N}_w'' + \mathbf{N}_w''^T \mathbf{N}_w'' \mathbf{q}_e \mathbf{N}_u' + \mathbf{N}_w''^T \mathbf{N}_u' \mathbf{q}_e \mathbf{N}_w'' \right) \right] d\xi + \\ & \int_0^1 \left[\frac{EI_0}{2l_e^2} \left(\mathbf{N}_u'^T \mathbf{N}_\theta' \mathbf{q}_e \mathbf{N}_\theta' + \mathbf{N}_\theta'^T \mathbf{N}_\theta' \mathbf{q}_e \mathbf{N}_u' + \mathbf{N}_\theta'^T \mathbf{N}_u' \mathbf{q}_e \mathbf{N}_\theta' \right) \right] d\xi + \\ & \int_0^1 \left[\frac{EI_0 - GI_0}{2l_e^3} \left(\mathbf{N}_\theta'^T \mathbf{N}_v' \mathbf{q}_e \mathbf{N}_w'' + \mathbf{N}_v'^T \mathbf{N}_w'' \mathbf{q}_e \mathbf{N}_\theta' + \mathbf{N}_w''^T \mathbf{N}_\theta' \mathbf{q}_e \mathbf{N}_v' \right) \right] d\xi - \\ & \int_0^1 \left[\frac{EI_0 - GI_0}{2l_e^3} \left(\mathbf{N}_\theta'^T \mathbf{N}_v'' \mathbf{q}_e \mathbf{N}_w' + \mathbf{N}_v''^T \mathbf{N}_w' \mathbf{q}_e \mathbf{N}_\theta' + \mathbf{N}_w'^T \mathbf{N}_\theta' \mathbf{q}_e \mathbf{N}_v'' \right) \right] d\xi \end{aligned} \tag{19}$$

Matrices $\mathbf{M}^{(e)}$ and $\mathbf{K}_e^{(e)}$ are the common mass and elastic stiffness matrices for a typical Bernoulli-Euler element. It is clear that use of a simplified expression of the non-linear part of the strain energy leads to an absence of several terms in the geometric stiffness matrix $\mathbf{K}_g^{(e)}$ of the element; however, the main contributions to the axial-bending-twisting coupling are retained. It has to be mentioned that in the derivation of the gyroscopic terms, it is assumed an approximation of a constant mean rotation velocity ω^e in the element. This assumption simplifies considerably the obtention of the gyroscopic terms.

Now, performing the conventional steps of assembling the finite elements, one obtains the following discrete equation of motion.

$$\mathbf{M}\,\ddot{\mathbf{q}} + \mathbf{G}\,\dot{\mathbf{q}} + \left[\mathbf{K}_e + \mathbf{K}_g\left(\mathbf{q}\right) \right] \mathbf{q} = \mathbf{F}_g \tag{20}$$

where $\mathbf{M}$, $\mathbf{G}$, $\mathbf{K}_e$, and $\mathbf{K}_g$ are the global mass matrix, gyroscopic matrix, elastic stiffness matrix, geometric stiffness matrix, respectively whereas $\ddot{\mathbf{q}}$, $\dot{\mathbf{q}}$, $\mathbf{q}$ and $\mathbf{F}_g$ are the global vectors of acceleration, velocities, displacements and gravity forces.

2.3 Analysis about an initially deformed configuration

In order to analyze the dynamics of the coupled axial/bending/torsional vibrations of the drill-strings, it is important to consider previously some aspects of the drilling process with the scope to characterize the FEM procedure. Drill-strings, such as the ones employed in oil well drilling can be represented by a vertical cylinder with fixed axial an lateral motion at the top position and sliding down due to own weight at the bottom location (i.e the drill bit). When the drill bit reaches the rock formation, a reaction acts at the bottom position. This reaction is considered time-invariant in the present work. At this stage the drill-string starts its rotational motion. Figure 1(b) and Figure 1(c) represent, respectively, the idealized undeformed and deformed configurations of the drill-string. In these circumstances four ”a posteriori” forces are included in the finite element model. Then, in addition to the gravity force vector $\mathbf{F}_g$ present in equation (18), at the bottom node is applied a force $\mathbf{F}_s$ to simulate the static axial reaction due to rock formation. Notice that in this work $\mathbf{F}_g$ and $\mathbf{F}_s$ are assumed time-invariant. Four external forces are added to the drill-string, namely a contact force $\mathbf{F}_C$ to simulate the structure-rock impacts, a friction force $\mathbf{F}_F$ related to the contact force $\mathbf{F}_C$, a perturbation force $\mathbf{F}_P$ due to induced lateral vibrations related to the contact of the drill-bit rock formation and a reactive torque T_{bit} is applied through the external generalized force vector $\mathbf{F}_T$.

Therefore, considering the aforementioned background, equation (20) can be rewritten in the following form:

$$\mathbf{M}\,\ddot{\mathbf{q}} + \mathbf{G}\,\dot{\mathbf{q}} + [\mathbf{K}_e + \mathbf{K}_g\,(\mathbf{q})]\,\mathbf{q} = \mathbf{F}_g + \mathbf{F}_s + \mathbf{F}_C + \mathbf{F}_P + \mathbf{F}_T + \mathbf{F}_F \tag{21}$$

In this work, it is supposed that after the quasi-static lowering and when the reaction force reaches a prescribed value, then further motions take place around this initial deformed configuration, which is obtained from the following equation:

$$\mathbf{q}_s = \mathbf{K}_e^{-1}\,(\mathbf{F}_g + \mathbf{F}_s) \tag{22}$$

this static configuration holds because the force vectors $\mathbf{F}_C$, $\mathbf{F}_P$, $\mathbf{F}_T$ and $\mathbf{F}_T$ are initially zero.

It has to be pointed out that equation (22) was obtained assuming that the terms of geometric stiffness matrix are negligible compared to those of the elastic stiffness matrix for the initial axial loading (Trindade et al., 2005). Then, defining a new displacement vector $\bar{\mathbf{q}}$ relative to the static $\mathbf{q}_s$, as

$$\bar{\mathbf{q}} = \mathbf{q} - \mathbf{q}_s \tag{23}$$

substituting $\mathbf{q}$ from equation (23) into equation (21) and taking into account equation (22), it is possible to obtain the following equations of motion (24) in terms of $\bar{\mathbf{q}}$, i.e in terms of the relative displacement vector:

$$\mathbf{M}\,\ddot{\bar{\mathbf{q}}} + \mathbf{G}\,\dot{\bar{\mathbf{q}}} + [\mathbf{K}_e + \mathbf{K}_g\,(\bar{\mathbf{q}} + \mathbf{q}_s)]\,\bar{\mathbf{q}} = \mathbf{F}_C + \mathbf{F}_P + \mathbf{F}_T + \mathbf{F}_F \tag{24}$$

Then, the axial displacement of the drill-bit is locked into its static value, that is: $\bar{u}^{(L)} = 0$ or $u = u_s^{(L)}$, the lateral displacement of drill-bit are locked as well (i.e. $\bar{v}^{(L)} = 0$ and $\bar{w}^{(L)} = 0$). On the other hand the top position of the drill-string is subjected to a constant rotary speed Ω, and the other displacements and rotations are locked. Notice that the boundary conditions at top of the drill-string and at the drill-bit conform a type of clamped-hinged beam.

The reactive torque is applied at the bottom node N, i.e. in the $(6N)^{th}$ degree of freedom of the vector $\mathbf{F}_T$, and it can be defined by means of following simplified form (Tucker and Wang, 2003), which takes into account the Coulomb frictional effect:

$$T_{bit} = \alpha_T F_{bit} \left[\frac{\dot{\theta}^3_{x_{bit}}}{\left(\dot{\theta}^2_{x_{bit}} + \kappa^2\right)^2} \right] \tag{25}$$

where F_{bit} is the static reaction, α_T is a coefficient (with dimensions [m s^{-1}]) which can be obtained from drill-string operational measurements. The coefficient κ is employed to approximate the Coulomb friction characteristics. It can have the value $\kappa = 2$ rad/seg Trindade and Sampaio (2005).

The contact force vector $\mathbf{F}_C$ is composed of nodal impact forces F^i_C that depend on whether the node i^{th} node is in contact or not with the borehole. These forces are calculated by means of the following law:

$$F^i_C(t) = \begin{cases} 0, & \forall \sqrt{(v^i)^2 + (w^i)^2} \leq \chi \\ -k\left[\sqrt{(v^i)^2 + (w^i)^2} - \chi\right], & \forall \sqrt{(v^i)^2 + (w^i)^2} > \chi \end{cases} \tag{26}$$

where k is a spring constant to simulate the impact force, $\chi = (D_H - D_e)/2$ is the gap between the borehole surface and the surface of the drill-string, $\sqrt{(v^i)^2 + (w^i)^2}$ is the displacement of the drill-string in the radial direction. Notice that expression (26) corresponds to the force in the radial direction, therefore it has to be appropriately projected in the y-direction and z-direction. Now related to the presence of contact one can also simulate in the following simplified form the friction force $\mathbf{F}_F$:

$$F^i_F = -\mu k \left[\sqrt{(v^i)^2 + (w^i)^2} - \chi\right] Sign\left[\dot{\theta}^i_x\right] \tag{27}$$

where μ is a type of friction coefficient and $\dot{\theta}^i_x$ is the velocity of rotation of the cross-section in the i^{th} node of contact. Notice that this force, acting tangentially to the cylindrical surface of the drill-string, gives three component to the nodal vector of forces, i.e. the projections in the y-direction and z-direction, and the friction torque

The perturbation due to induced lateral vibrations can be simulated by means of a sinusoidal bending moment related to static reaction force F_{bit} and applied in the hinged location varying with a certain frequency and as the drill-bit is rotates. Thus the expression of the perturbation moment is:

$$\begin{aligned} M_{y_{bit}} &= \alpha_M F_{bit} Sin\left[\Omega_P t\right] Sin\left[\theta_{x_{bit}}\right] \\ M_{z_{bit}} &= \alpha_M F_{bit} Sin\left[\Omega_P t\right] Cos\left[\theta_{x_{bit}}\right] \end{aligned} \tag{28}$$

In equation (28), α_M (with dimensions in [m]) is a factor of proportionality that magnifies the influence of the perturbation for a determined Force on bit depending on the type of rock formation under drilling. Ω_P is the perturbation frequency.

The equation (24) can be modified to account for structural damping, that is:

$$\mathbf{M}\,\ddot{\bar{\mathbf{q}}} + \left(\mathbf{G} + \mathbf{C}_{RD}\right)\dot{\bar{\mathbf{q}}} + \left[\mathbf{K}_e + \mathbf{K}_g\left(\bar{\mathbf{q}} + \mathbf{q}_s\right)\right]\bar{\mathbf{q}} = \mathbf{F}_C + \mathbf{F}_P + \mathbf{F}_T \tag{29}$$

The matrix $\mathbf{C}_{RD}$ corresponds to the system proportional Rayleigh damping given by:

$$\mathbf{C}_{RD} = \alpha\mathbf{M} + \beta\mathbf{K}_e \tag{30}$$

where $\mathbf{M}$ and $\mathbf{K}_e$ are the global mass and elastic stiffness matrices, respectively; whereas parameters α and β are computed from two experimental modal damping functions (Bathe, 1982; Meirovith, 1997). Notice that the damping matrix is referred to the linear component of the stiffness matrix.

The Matlab program is employed to simulate numerically the finite element model, for this reason the equation (29) is represented in the following ODE form:

$$\mathbf{A}\frac{d\mathbf{W}}{dt} + \mathbf{B}\mathbf{W} = \mathbf{0} \tag{31}$$

where:

$$\mathbf{A} = \begin{bmatrix} \mathbf{C}_{RD} + \mathbf{G} & \mathbf{M} \\ \mathbf{M} & \mathbf{0} \end{bmatrix}, \mathbf{B} = \begin{bmatrix} \mathbf{K}_e + \mathbf{K}_g(\mathbf{q}) & \mathbf{0} \\ \mathbf{0} & -\mathbf{M} \end{bmatrix}, \mathbf{W} = \left\{ \bar{\mathbf{q}}, \frac{d\bar{\mathbf{q}}}{dt} \right\}^T \tag{32}$$

Taking into account that the problem includes vibroimpacts and other non-linear nodal loadings, and the numerical model can be stiff hence hard to integrate, therefore the solver "ode15s" for integration of stiff systems is employed.

3 NUMERICAL ANALYSIS

In this and the following subsections, the dynamics of a typical drill-string is simulated by means of the non-linear finite element formulation introduced in the previous sections. The material and geometric properties of the drill-string are adapted from the open technical literature (Trindade et al., 2005). These properties are shown in Table 1. For simplification purposes, the drill-string is divided in two different segments as shown in Figure 1. The upper segment is composed of drill pipes, which are subjected to traction forces. On the other hand the lower segment is composed by strong and heavy pipes which are subjected to compression by the weight of the upper segment and the reaction force of the rock-formation. The lower pipes are thus subjected to an intense bending-axial-torsional coupling.

The drill-string is confined in a borehole with diameter $D_H = 0.312$ m. and two stabilizers were located at 20 m and 40 m from the drill-bit. In the finite element model, the stabilizers are accounted for by locking the transversal degrees of freedom at their corresponding locations (i.e. 1980 m and 1960 m from rotary table) in the finite element model.

Property	Section 1	Section 2
Longitudinal Elastic Modulus E (GPa)	210	210
Transversal Elastic Modulus G (GPa)	80	80
Mass density ρ (kg/m^3)	7850	7850
Internal Diameter D_I (m)	0.108	0.076
External Diameter D_E (m)	0.128	0.204
Length (m)	1800	200
Bore-hole Diameter D_H (m)	0.312	0.312

Table 1: Geometrical and Material properties of the drill string

In the present paragraph for simulation and analysis purposes the coefficients related to the perturbation, contact and the other forces have the following values: $\alpha_T = 0.1$, $\alpha_M = 0.1$. The frequency of perturbation in equation (28) is assumed $\Omega_P = 2\pi$. The spring constant for contact and friction forces is $k = 1 \times 10^8$ N/m. The drill-string is lowered until a static reaction force of 20% of the weight of the BHA is reached at the bit (remember that this reaction force is considered time-invariant in the present work). Then, the top position is subjected to a constant rotation velocity of $\Omega = 10$ rad/seg. The coefficients α and β are calculated (Bathe, 1982) assuming for simulation purposes the damping coefficients $\xi_1 = 10^{-4}$ and $\xi_2 = 2 \times 10^{-4}$ for the first and second frequencies respectively. The finite element models employed have 144 degrees of freedom, which was observed to represent appropriately the dynamic response.

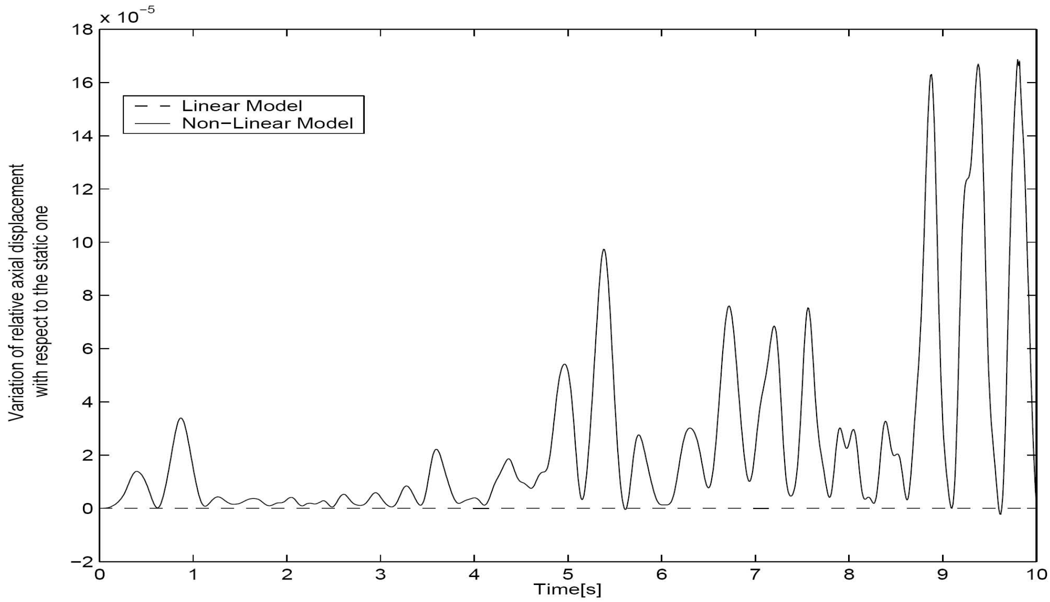

Figure 3: Variation of the relative axial displacement with respect to the static one $\bar{u}^{(m)}/u_s(m)$ measured at the position $x_m = 1993.33$ m, using linear and non-linear model for a bottom reaction force of 20% of the BHA weight (i.e. $F_{bit} = 86700$ N)

The time-history of the relative axial displacement at position $x_m = 1993.33$ m (i.e. 6.67 m from the drill-bit) with respect to the axial static displacement is shown in Figure 3, for both the linear and non-linear models. The force on bit is fixed at the 20% of the BHA weight. One can see that the axial displacement in the case of linear model maintains its value during the period under study. This behavior is due to the fact that there is no coupling between the axial displacement and flexural-torsional displacements which are in fact the excited displacements. On the other hand one can see a variation of the axial displacement for the non-linear model because it is excited by means of the coupling of transversal and torsional displacements. Although much smaller than the static displacement (for this reason it is normally neglected), the effect of the variation of the axial displacement relative to the static is relevant for the calculation of the forces, that will be shown later in next paragraphs.

Figure 4 shows, for the linear and non-linear models, the time variation of the radial displacement of a section located at the position $x_m = 1993.33$ m from the top. The figure also shows the borehole clearance in order to see when the surface of the drill-string impacts with the rock. It is possible to see that after a brief transition period the non-linear model starts the

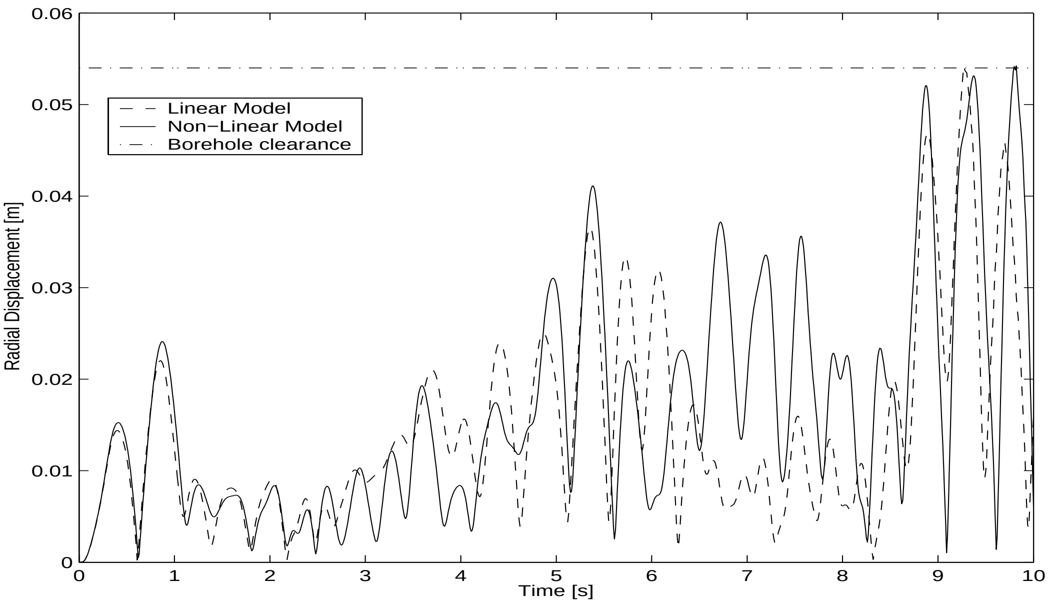

Figure 4: Variation of the displacement of the cross section in the radial direction, measured at the position $x_m = 1993.33$ m, using linear and non-linear model for a bottom reaction force of 20% of the BHA weight (i.e. $F_{bit} = 86700$ N)

impacts with the borehole before the linear model.

Figure 5 and Figure 6 show the same information of the Figure 3 and Figure 4, respectively, but for a force on bit of 30 % of the BHA weight. In Figure 6, one can observe that an intense impact pattern begins rapidly after the first few seconds in the non-linear model, whereas in the linear model the impacts begins after the non-linear and appears to be not too severe and quite similar to the case where the force on bit is of 20 % of the BHA weight.

It is also interesting to study the effect of the coupling between axial, flexural and torsional vibration, in the calculation of reaction forces. In the Figure 7 one can see the variation of the reaction force at the top position for the linear and non-linear models, for the case in which the force on bit is fixed at the 30 % of the BHA weight. A comparison between both responses shows that the linear model for which the axial, flexural and torsional motions are uncoupled, can not capture the vibrations transmitted from the perturbation moments acting in the bottom. Only the static force due to the drilling weight can be captured by the linear model. On the other hand the non-linear model can describe well the variation of the reaction force at the top position. Although the static and the dynamic patterns of the reaction force at the top, do not present a sensible quantitative difference, the qualitative difference is important in order to consider control techniques, for example to maintain a determined force on bit as the drilling process evolves.

4 CONCLUSIONS

In the present work, the non-linear vibrations of a rotating drill-string represented by a vertical slender annular beam were studied. The beam was clamped in its upper extreme and pinned in its lower extreme, and it was constrained to move inside a cylinder simulating the rock formation. This confinement of the lateral motions leads to a number of vibroimpacts, especially in lower part of the drill-string. The beam is subjected to its own weight. These forces lead to geometric stiffening in the upper part of the drill-string, i.e. in the slender pipes, however,

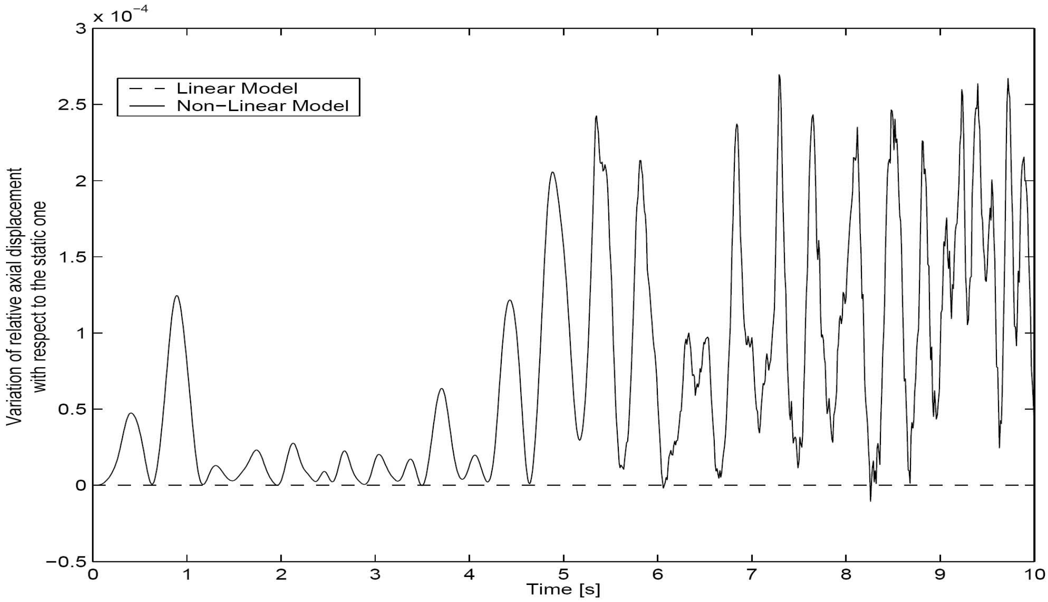

Figure 5: Variation of the relative axial displacement with respect to the static one $\bar{u}^{(m)}/u_s(m)$ measured at the position $x_m = 1993.33$ m, using linear and non-linear model for a bottom reaction force of 30% of the BHA weight (i.e. $F_{bit} = 144500$ N)

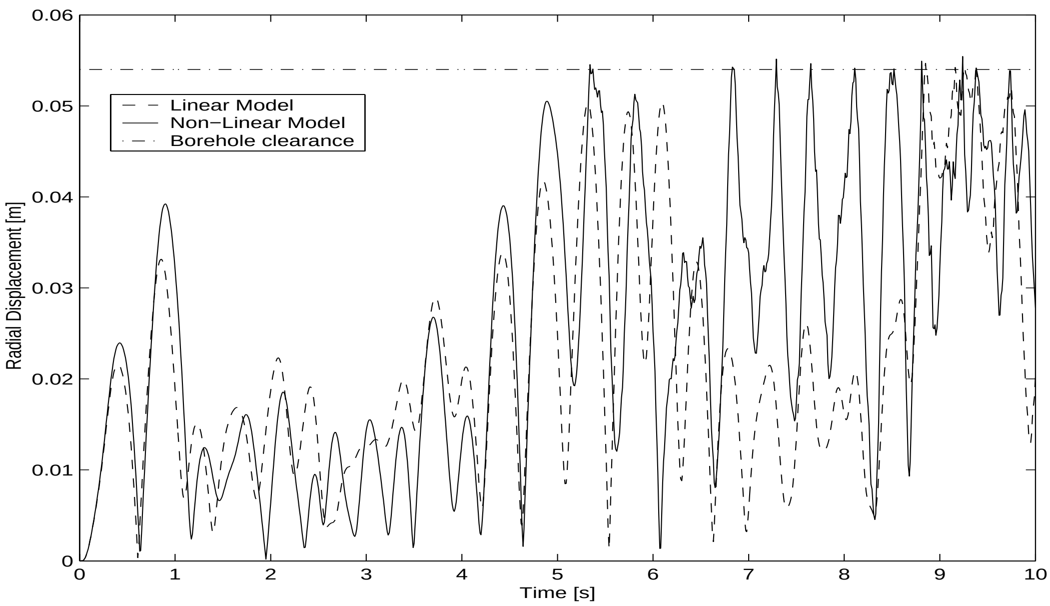

Figure 6: Variation of the displacement of the cross section in the radial direction, measured at the position $x_m = 1993.33$ m, using linear and non-linear model for a bottom reaction force of 30% of the BHA weight (i.e. $F_{bit} = 144500$ N)

in its lower part, the Bottom Hole Assemblies, the drill-string presents a geometric softening effect due to the compression. The effects of impact, rock-structure friction and other factors of perturbation in the drill-string were considered. These interactions were modeled in a simplified fashion, but although one could also consider a more sophisticate interaction model to account for inelastic impacts and the other perturbation effects, the interest of the present work

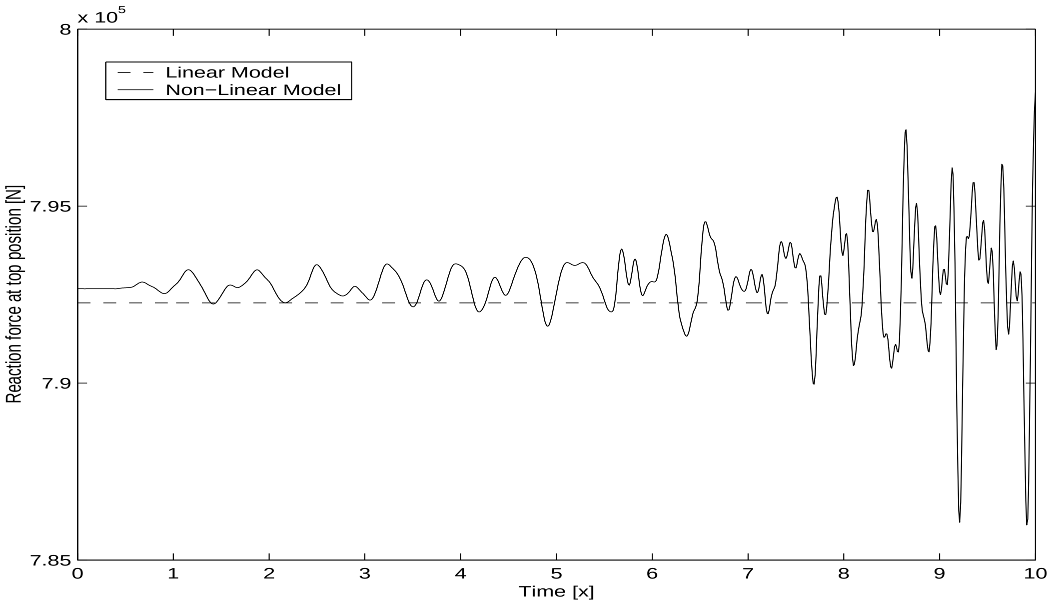

Figure 7: Variation of the Radial Transversal displacement measured at the position $x_m = 1993.33$ m, using linear and non-linear model for a bottom reaction force of 30% of the BHA weight (i.e. $F_{bit} = 144500$ N)

was focused in the evaluation of the geometric non-linearities in the dynamics of drill-strings formulated by means of general continuous rotating beams. One can see that the impact patterns and the reaction forces are well described only when the non-linear model is used, especially when the force on bit reaches high values, which implies in essence a better drilling performance, but with a substantial increase in the number of impacts.

5 ACKNOWLEDGEMENTS

This work was supported by CNPq, Project 470814/2003-9, Universidad Tecnologica Nacional, Facultad Regional Baha Blanca and CONICET.

REFERENCES

K.J. Bathe. *Finite Element procedures in Engineerign Analysis*. Prentice-Hall, Englewood Cliffs, New Jersey, 1982.

A. Berlioz, J. Der Hogopian, R. Dufour, and E. Draoui. Dynamic behavior of a drillstring: experimental investigation of lateral instabilities. *Journal of Vibration and Acoustics*, 118: 292–298, 1996.

S.L. Chen and M. Géradin. An improved transfer matrix technique as applied to bha lateral vibration analysis. *Journal of Sound and Vibration*, 185:93–106, 1995.

A.P. Christoforou and A.S. Yigit. Fully coupled vibrations of activelly controlled drillstrings. *Journal of Sound and Vibration*, 267:1029–1045, 2003.

H.B.H. Gubran and K. Gupta. The effect of stacking sequence and coupling mechanisms on the natural frequencies of composite shafts. *Journal of Sound and Vibration*, 282:231–248, 2005.

J.D. Jansen. Non-linear rotordynamics as applied to oil-well drillstring vibrations. *Journal of Sound and Vibration*, 147:115–135, 1991.

J.D. Jansen and L. van den Steen. Active damping on self-excited torsional vibrations of oil well drill-string. *Journal of Sound and Vibration*, 179:647–668, 1995.

Y.A. Khulief and H. Al-Naser. Finite element dynamic analysis of drillstrings. *Finite elements in analysis and design*, 41:1270–1288, 2005.

M. Lalanne and G. Ferraris. *Rotordynamics Prediction in Engineering*. John Wiley and Sons, Chichester, West Sussex, England, 1990.

L. Meirovith. *Principles and Techniques of Vibrations*. Prentice Hall, Upper Saddle River, New Jersey, 1997.

H. Melakhessou, Berlioz A., and G. Ferraris. A non-linear well-drillstring interation model. *Journal of Vibration and Acoustics*, 125:46–52, 2003.

M.A. Mohiuddin and Y.A. Khulief. Coupled bending torsional vibration of rotors using finite element. *Journal of Sound and Vibration*, 223:297–316, 1999.

T. Richard, C. Germay, and E. Detournay. Self-excited stick-slip oscillations of drill-bit. *Comptes Rendus Mécanique*, 332:619–626, 2004.

R. Sampaio, M.T. Piovan, and G. Venero. *Non-linear model for coupled axial/torsional vibrations of drill-strings*. Proceedings of 18^{th} International Congress of Mechanical Engineering, ABCM, 2005.

M.A. Trindade and R. Sampaio. *Modeling of axial-torsional coupled vibrations of drill-strings.* 13^{th} International Workshop on Dynamics and Control, Daimler–Chrysler Training Center, Wiesenteig, Germany, Shaker Verlag, 2005.

M.A. Trindade, C. Wolter, and R. Sampaio. Karhunen-loève decomposition of coupled axial/vending vibrations of beams subject to impacts. *Journal of Sound and Vibration*, 279: 1015–1036, 2005.

R.W. Tucker and C. Wang. An integrated model for drill-string dynamics. *Journal of Sound and Vibration*, 32:2223–2241, 1999.

R.W. Tucker and C. Wang. Torsional vibrations control and cosserat dynamics of a drill-rig assembly. *Meccanica*, 38:143–159, 2003.

A.S. Yigit and A.P. Christoforou. Coupled torsional and bending vibrations of drillstrings subjected to impact with friction. *Journal of Sound and Vibration*, 215:167–181, 1998.

A.S. Yigit and A.P. Christoforou. Coupled bending and torsional vibrations of activelly controlled drillstrings. *Journal of Sound and Vibration*, 234:76–83, 2000.